Innovative Food Science and Emerging Technologies 68 (2021) 102628

Contents lists available at ScienceDirect

Innovative Food Science and Emerging Technologies

journal homepage: www.elsevier.com/locate/ifset

A simplified approach to assist process development for microwave assisted pasteurization of packaged food products

Yoon-Ki Hong [a], Frank Liu [a], Zhongwei Tang [a], Patrick D. Pedrow [b], Shyam S. Sablani [a], Ren Yang [a], Juming Tang [a,*]

[a] Department of Biological Systems Engineering, Washington State University, P.O. Box 646120, Pullman 99164, USA
[b] School of Electrical Engineering & Computer Science, Washington State University, P.O. Box 642752, Pullman 99164, USA

ARTICLE INFO

Keywords:
Microwave heating
Heat penetration
Analytical method
Process development

ABSTRACT

The purpose of this study was to develop a convenient method to assist the food industry in developing process schedules for production of ready-to-eat meals using microwave assisted pasteurization system (MAPS). An analytical model was applied to estimate the temperature increase in the cold zone in packaged foods during heating in a 915 MHz single-mode microwave system. This model was validated in a pilot-scale four-cavity MAPS using mashed potato-gellan gum model food with different thicknesses (22 to 36 mm) and salt contents (0.0 to 1.0%). Mobile sensors were placed in the packages to measure temperature at the pre-determined cold spots. For 2.48 min of microwave heating with 5, 5, and 8.7 kW 915 MHz microwave powers, the highest temperature increase at the cold spot during microwave heating was 33.2 °C in the 22 mm thick model food with 0.6% salt content, whereas the lowest temperature increase was 10.3 °C in the 36 mm thick model food with 1.0% salt content. There was a deviation of 1.9 ± 1.2 °C between experimental and predicted data with an R^2 of 0.89. A simplified chart was developed based on the validated analytical results to allow rapid prediction of temperature increases in MAPS as influenced by food dielectric properties and package thickness. Examples were used to illustrate how the chart could assist in process scheduling. The chart can help assess the heating rates of various pre-packaged food products in a specific industrial MAPS or guide product development for desired heating uniformity.

1. Introduction

Interest in emerging technologies, including non-thermal and thermal processing for ready-to-eat meals, is drastically increasing with increased consumer concerns about food safety issues and demands for high-quality products (Dolores Alvarez, Herranz, Campos, & Canet, 2017; Moreno-Vilet, Hernández-Hernández, & Villanueva-Rodríguez, 2018). Microwave heating, one of the emerging technologies, has been extensively studied over the past several decades. Properly designed microwave systems are able to produce safe and high-quality pre-packaged ready-to-eat meals (Huang & Sites, 2010; Tang, 2015; Tang, Hong, Inanoglu, & Liu, 2018). As a volumetric heating method, microwave heating provides shorter processing time and more uniform heating as compared to conventional heating methods such as retort or hot-water processing (Chandrasekaran, Ramanathan, & Basak, 2013; Tang et al., 2018).

In the USA, 915 and 2450 MHz microwave frequencies are allocated by the Federal Communications Commission (FCC) for industrial, scientific, and medical (ISM) applications. 2450 MHz microwaves are used in domestic ovens and also in industrial heating (Orsat, Raghavan, & Krishnaswamy, 2017; Tang et al., 2018). The heating chambers of 2450 MHz microwave systems are often designed as multi-mode cavities, leading to complex and unpredictable electromagnetic fields (Tang, 2015). Furthermore, variations in the location, the shapes and properties of products can change the heating patterns and the cold spots in a 2450 MHz multi-mode cavity (Chandrasekaran et al., 2013; Luan, Wang, Tang, & Jain, 2017; Soto-Reyes, Temis-Pérez, López-Malo, Rojas-Laguna, & Sosa-Morales, 2015). Stability of cold spot locations in pre-packaged food is imperative for industrial-scale pasteurization and sterilization systems in order to ensure microbial safety of processed food. For heat-based processing including microwave heating, the United States Food and Drug Administration (FDA) requires the heating penetration tests with temperature measurement at the determined cold spot when validating industrial processes (FDA, 2016).

* Corresponding author at: Biological Systems Engineering, Washington State University, P.O. Box 646120, Pullman, WA 99164-6120, USA.
E-mail address: jtang@wsu.edu (J. Tang).

https://doi.org/10.1016/j.ifset.2021.102628
Received 30 November 2020; Received in revised form 21 January 2021; Accepted 22 January 2021
Available online 26 January 2021

Through decades of collaborative research with food and equipment companies, a new system design that combines microwave heating in 915 MHz single-mode microwave cavities with high temperature circulating water has been developed to provide predictable heating patterns in pre-packaged foods. The unique features of this design are discussed in detail in Tang (2015). The first microwave assisted thermal sterilization (MATS) system with a capacity of 30 meals per min was installed by Tata SmartFoodz (Chennai, India) in 2019 for commercial production of shelf-stable meals. In 2020, additional MATS systems with larger capacities have been installed at Tata Smartfoodz, more are planned for other companies in different countries. The same concept for 915 MHz single-mode cavity design was recently used in the development of microwave assisted pasteurization systems (MAPS) for control of bacterial and viral pathogens in chilled or frozen ready-to-eat meals (Tang et al., 2018). MAPS are intended mostly for small and medium-sized food companies that may not have adequate engineering and R&D capacities. There is a need for effective, simple, and convenient tools to assist plant engineers to develop MAPS process schedules for various types of products and package geometries.

Fig. 1 shows the schematic design of the pilot-scale MAPS installed at Washington State University (Pullman, WA, USA). The system consists of four sections: pre-heating, microwave heating, holding, and cooling. In operation, food packages in metal frame carriers are first heated in the pre-heating section to reach a uniform temperature before being transported to the microwave heating section. In the microwave heating section, the food temperature rapidly increases to a target pasteurization temperature (Tang, 2015). The packages are then transported through the holding section to obtain a certain lethality at the cold spot, and finally, moved into the cooling section. The microwave heating section consists of four 915 MHz single-mode cavities filled with hot circulating water of low electric conductivity. Here, the food packages immersed in the water are heated by a combination of volumetric microwave heating and surface water heating. This combination offers predictable heating patterns without edge heating that is commonly observed in domestic microwave ovens. 915 MHz microwaves have a longer wavelength (0.33 m in the air) which provides more uniform heating inside food packages when compared with 2450 MHz microwaves (with a wavelength of 0.12 m in the air). Thus, the 915 MHz single-mode cavity design is more suitable to heat packaged meals with various shapes and thicknesses than the 2450 MHz multi-mode cavity design for industrial applications (Tang, 2015). Previous tests on green bean and garlic based model foods in MAPS showed shorter process times and better food qualities than conventional heating at the same lethality (Bornhorst, Tang, Sablani, Barbosa-Canovas, & Liu, 2017). Pasta processed with the MAPS showed a similar sensory test result when compared to home-cooked pasta (Joyner, Jones, & Rasco, 2016).

The shelf-life of the pasteurized products is determined by the process conditions for MAPS. For example, food processed to 70 °C and held for 2 min are expected to have a 10-day shelf-life when stored at less than 5 °C, while food processed to 90 °C and held for 10 min have a shelf-life of 6 weeks at the same storage temperature (Peng et al., 2017). In MAPS process development, the heating rate is governed by several factors including thermal properties, dielectric properties, and thicknesses of the food. The ability to predict how fast and uniformly food can be heated in MAPS should help in the selection of appropriate parameters such as microwave power, conveyor speed, vessel temperature, processing time.

Over the last decades, computer simulation has been used to simulate electric fields in 915 MHz single-mode cavities of MATS system or MAPS (Chen, Tang, & Liu, 2006, 2008; Jain, Tang, Liu, Tang, & Pedrow, 2018; Luan, Tang, Pedrow, Liu, & Tang, 2013; Luan, Tang, Pedrow, Liu, & Tang, 2015; Luan, Tang, Pedrow, Liu, & Tang, 2016; Resurreccion et al., 2013; Resurreccion et al., 2015). In those simulation studies, the finite-difference time-domain (FDTD) method was used to determine three-dimensional (3-D) heating patterns in food packages moving through microwave cavities (Jain et al., 2018; Luan et al., 2016; Resurreccion et al., 2013). The simulation results were validated by experiments using a computer vision method (Pandit, Tang, Liu, & Mikhaylenko, 2007). While the simulation provided very useful insight into key issues related to the stability of heating patterns and cold spot, and about the suitability of using mobile sensors for accurate temperature measurement at the cold spots, the simulation work requires high-performance computers and long calculation time for the industrial-scale continuous processes (Jain et al., 2019; Resurreccion et al., 2013). Furthermore, specialized knowledge is necessary to develop the numerical models and to interpret the results, because of the complex physical processes involving food carrier movement, microwave propagation, and heat transfer phenomena. Food companies, in particular small- and medium-sized companies, generally lack such knowledge and related expertise.

Alternatively, analytical approaches can be applied to develop a general understanding of microwave heating of various food products (Ayappa, Davis, Crapiste, Davis, & Gordon, 1991; Hossan, Byun, & Dutta, 2010; Jain et al., 2019; Van Remmen, Ponne, Nijhuis, Bartels, & Kerkhof, 1996; Yang & Gunasekaran, 2001). Jain et al. (2019) developed an analytical model from Maxwell's equations to help the process schedule development for MATS processing. The derived model was validated using pea, rice, and mashed potato-based foods that presented relatively large ranges of physical properties for food products (e.g., volumetric specific heat, dielectric constant, and loss factor). The analytical model is useful in assessing the influence of food properties and package thickness on the heating rates at the cold spots in food packages during heating in 915 MHz single-mode cavities.

Heating rate is an essential parameter in the development of schedules for MAPS processing of packaged food products. It is closely correlated with microwave field intensity in food, as well as the dielectric properties and thickness of the food product. The interaction

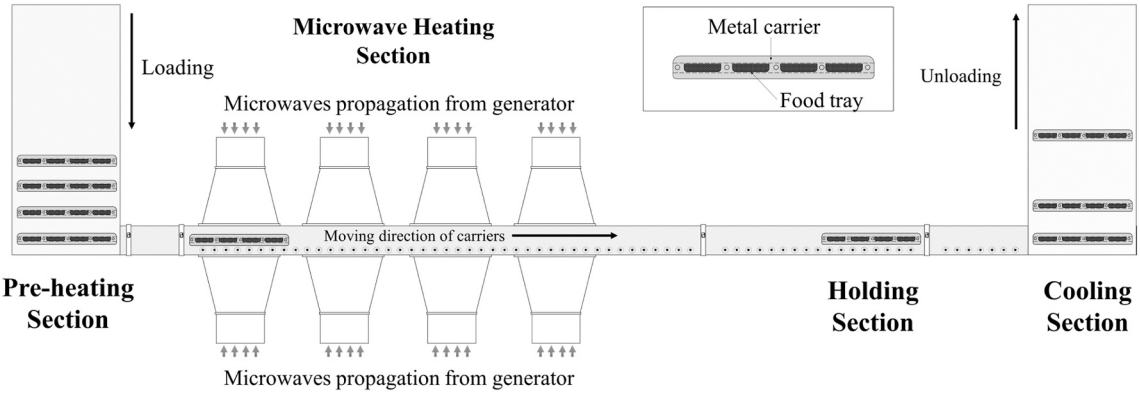

Fig. 1. Schematic design of Microwave Assisted Pasteurization System (MAPS).

between food and electromagnetic waves is mainly governed by dielectric properties of the food, which affects the dissipation of microwave energy (Chandrasekaran et al., 2013). The thickness of food affects the power intensity of the microwaves that penetrate to the middle layer of the food. The heating rate in the microwave heating strongly affects the final product temperature and energy efficiency of a system. Developing a tool for heating rate prediction could guide manufacturers to estimate required processing time. This tool can also be used to select food components for relatively uniform heating, reduce process development time, and produce higher quality products.

The objectives of this research were to: 1) develop a simplified method based on an analytical model to estimate heating rates for MAPS processes; 2) to validate the analytical method with pilot-scale testing; and 3) to develop an effective tool that would assist food companies in process and producte development. Specifically, the analytical model developed by Jain et al. (2019) was applied to the MAPS to calculate the heating rates and temperature increments of food products in microwave heating. The analytical results were validated by comparing with the experimental results of heating patterns and temperature increases during the microwave heating in the pilot-scale MAPS. The validated analytical model was then used to develop a chart to allow for the estimation of temperature increases in MAPS as influenced by food dielectric properties and package thickness. Examples are included to illustrate how this chart could assist in the development of process schedules and food products.

2. Materials and methods

2.1. Mathematical models

2.1.1. Assumptions

In the MAPS, microwave heating is applied to the packaged foods while they pass through the microwave heating section (Fig. 1). The following assumptions were used to simplify the calculation of the temperature increase at the cold spot in pre-packaged food in the microwave heating section of the pilot-scale MAPS (Fig. 2).

i. The microwave heating section in the MAPS consists of four microwave applicators (Fig. 1). In each applicator, an equal amount of microwaves propagate in TE10 mode is applied through the top and bottom waveguides (Tang, 2015). The two streams of waves entered the cavity with a 0° phase difference and create standing waves within food packages located at the center of the cavity (Luan et al., 2016). The electromagnetic waves travel in the z-direction and have electric fields in the y-direction through the 915 MHz single-mode cavity (Fig. 2). We assumed that electromagnetic waves were incident normally on a rectangular food immersed in water from the top and bottom.
ii. Food products were solid and isotropic linear materials. Food materials generally behave non-magnetically, and the relative permeability (μ_r) was set to 1.
iii. The incident electric field intensity (E_0) is an important operational parameter used to calculate the temperature increase during microwave heating. The magnitude of E_0 was set 1 kV/m, which was obtained from a computer simulation model in previous studies (Jain et al., 2019; Luan et al., 2016). The chosen value was sufficient to model an energy distribution in food with various dielectric properties and thicknesses. However, a more precise E_0 with respect to a certain location (i.e., effective E_0 at a location, E_{0eff}) in food is required to estimate the actual heating rate in industrial systems. Based on the previous research on MATS systems, the cold spots are generally located in the center layer of foods because of concurrent surface heating by high-temperature circulation water in the microwave cavities (Luan et al., 2015; Resurreccion et al., 2015). Thus, the temperature increase was calculated at the selected cold point of the center

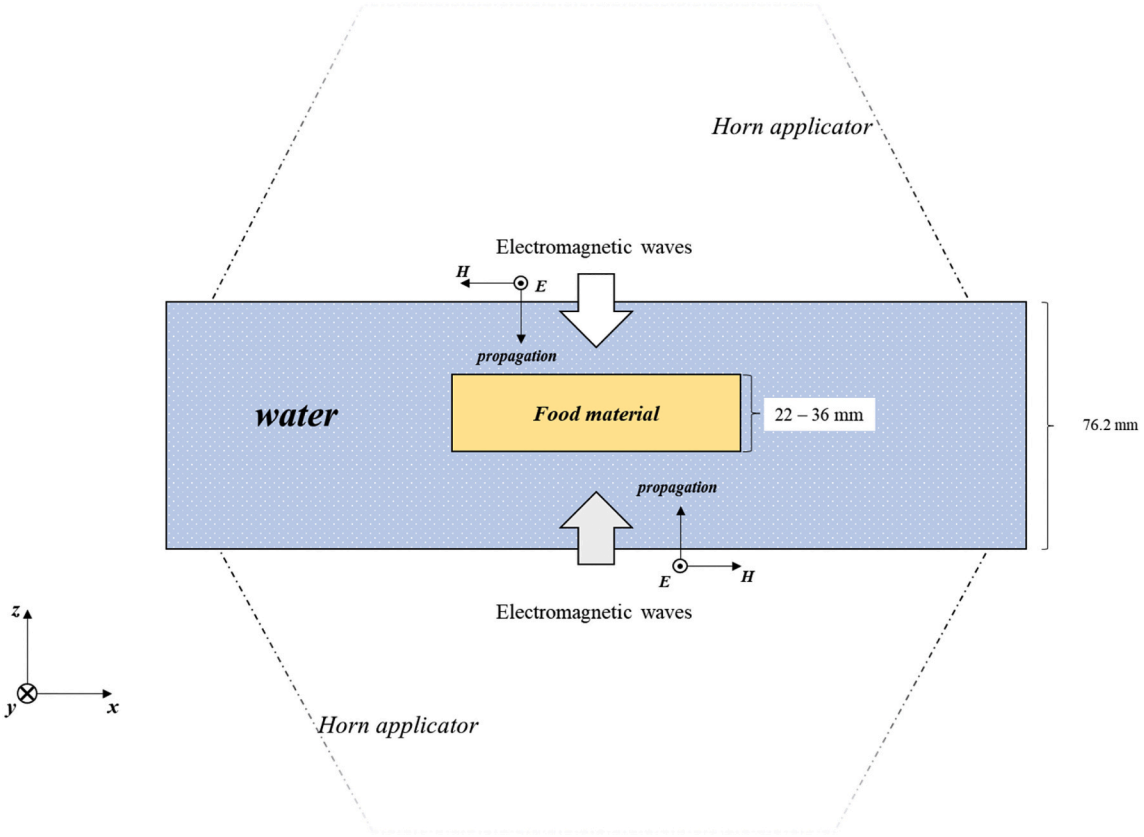

Fig. 2. Concept of analytical model for MAPS: microwave propagation in phase on top and bottom sides of rectangular food (modified from Jain et al. (2019)).

layer of the model food. The E_{0eff} of 0.527 kV/m at the center layer of model foods was reversely calculated from measured temperature increase in the microwave section in preliminary MAPS runs using 22-mm-thick model food with 0.6% salt content.

iv. The influence of heat transfer from the circulation water on the temperature increase at the cold spots was negligible because the volumetric heat by microwaves was much faster than thermal diffusion from the circulation water to the center of foods within the short microwave heating times (Jain et al., 2019). Therefore, only microwave heating was used to estimate the temperature increase in the microwave heating zone of the MAPS. The total length of the four horn applicators in the microwave heating section (Fig. 1) was used to calculate the microwave heating time in the MAPS based on the moving speed of the food packages.

2.1.2. Development of mathematical model

Based on the above assumptions, a 1-D simplified model derived from Maxwell's equations was applied to calculate the electric field intensity at the cold spot in the cross-section within a food product (Jain et al., 2019):

$$E = \frac{T_{w/f} E_0}{1 + R_{w/f}\, e^{-\gamma_f L}} \left(e^{-\gamma_f z} + e^{-\gamma_f (L-z)} \right) \tag{1}$$

where E is the electric field intensity (V/m) at the cold spot inside the food with a distance z (m) from the interface ($L/2$ is the center location of food), L is food thickness (m), $T_{w/f}$ is the transmission coefficient, $R_{w/f}$ is the reflection coefficient at normal incidence on the interface between water and food, and γ_f is the propagation constant in food. The two coefficients can be written as (Sadiku, 2014):

$$T_{w/f} = \frac{2\eta_f}{\eta_w + \eta_f} \tag{2}$$

$$R_{w/f} = \frac{\eta_f - \eta_w}{\eta_w + \eta_f} \tag{3}$$

where η_w and η_f are the complex intrinsic impedances $\sqrt{\mu_0/\varepsilon_0 \left(\varepsilon_r' - j\varepsilon_r''\right)}$ calculated using dielectric properties of water and food, respectively, μ_0 is permeability in free space, ε_0 is permittivity in free space, ε_r' is the relative dielectric constant and ε_r'' is the relative loss factor. The subscripts $_w$ and $_f$ denote water and food, respectively. The propagation constant (γ_f) is expressed as:

$$\gamma_f = \alpha + j\beta \tag{4}$$

where α is the attenuation constant and β is the phase constant. The are expressed as:

$$\alpha = \frac{2\pi f}{c} \sqrt{\frac{\varepsilon_r'}{2} \left(\sqrt{1 + \left(\frac{\varepsilon_r''}{\varepsilon_r'} \right)^2} - 1 \right)} \tag{5}$$

$$\beta = \frac{2\pi f}{c} \sqrt{\frac{\varepsilon_r'}{2} \left(\sqrt{1 + \left(\frac{\varepsilon_r''}{\varepsilon_r'} \right)^2} + 1 \right)} \tag{6}$$

where f is the frequency (Hz).

2.1.3. Temperature increase calculation

The derived equation (Eq. 1) for calculating the electric field inside the food was utilized to estimate the temperature and electric field. Obtained electric field intensity values were converted to the dissipated microwave power per unit volume ($P(z)$, W/m^3):

$$P(z) = 2\pi f \varepsilon_0 \varepsilon_r'' |E|^2 \tag{7}$$

A general form of heating transfer equation is given by:

$$\nabla \cdot k \nabla T + P(z) = \rho C_p \frac{\partial T}{\partial t} \tag{8}$$

where T is the temperature (°C), k is the thermal conductivity of the medium (W/m·°C), and ρC_p is the volumetric specific heat (MJ/m^3·°C). As mentioned in section 2.1.1, only the dissipated microwave power was considered for heating. The temperature increase (ΔT, °C) during microwave heating is calculated by Jain et al. (2019):

$$\Delta T = \frac{P(z)t}{\rho C_p} \tag{9}$$

where t is time for microwave heating (s).

2.2. Experimental validation

2.2.1. Sample preparation

Mashed potato-gellan gum model food (with 0, 0.5, and 1.0% salt level) was used in the validation tests. Its formula was modified from Bornhorst, Tang, Sablani, and Barbosa-Cánovas (2017). The model food was made from 3% mashed potato flakes (Oregon Potato Co., Pasco, WA, USA), 0.75% low acyl gellan gum (Modernist Pantry LLC., Eliot, ME, USA), 1% L-lysine (Acros Organics, Geel, Belgium), 2% D-fructose (Fisher Science Education, Nazareth, PA, USA), 0.15% calcium chloride (Macron Fine Chemicals, Randor, PA, USA), 0.4% titanium dioxide (Lorann oils Inc., Lansing, MI, USA), 92.7–91.7% distilled and deionized (DDI) water, and 0–1% table salt (Morton salt Inc., Chicago, IL, USA). Calcium chloride was used to strengthen the gel structure of the model food, and titanium dioxide was used as a white color agent, table salt was used to control the dielectric properties, and L-Lysine and D-fructose were used as a precursor of the M-1 chemical marker for determining heating patterns.

For sample preparation, the low acyl gellan powder was first mixed with DDI water. The mixture was heated in a beaker to 90 °C on a hot plate while stirring, and mashed potato flakes and calcium chloride were gradually added to the mixture. Then the mixture was cooled to 75–80 °C, salt and titanium dioxide were added. D-fructose and L-lysine were added after the mixture's temperature reached 65–75 °C. This well-mixed solution was finally poured into either 27 mm-thick (dimension: 95 × 140 × 27 mm, sample weight: 280, 310, and 340 g) and 36 mm-thick trays (dimension: 95 × 140 × 36 mm, sample weight: 430 g) at 65–75 °C. After cooling at room temperature (21 °C), the model food was sealed in trays and stored in a refrigerator (for less than 12 h) until testing.

2.2.2. Dielectric and thermal properties measurements

Dielectric properties of the model foods were measured using a network analyzer (HP 8752C, Hewlett-Packard, Palo Alto, CA, USA) with an open-end coaxial dielectric probe (85070B, Agilent Technologies, Santa Clara, CA, USA) at 25–100 °C (Wang, Wig, Tang, & Hallberg, 2003). The dielectric properties are shown in Fig. 3. Thermal properties of the model foods (ρC_p and k) were measured at 60–100 °C using KD2 Pro Thermal Properties Measurement Instrument (KD2 pro, Meter Group, Pullman, WA, USA). The average ρC_p of 3.706 MJ/(m^3·°C) was used to calculate ΔT. The average k was 0.60 at 60–100 °C. All measurements were replicated three times.

2.2.3. MAPS processing

The process conditions are described in Table 1. Process time and temperature of each section were set based on preliminary tests. Prepared model foods in sealed polymeric trays were processed while moving through the four cavities of the MAPS equipped with two 5 kW and one 8.7 kW microwave generators. The microwave power from the 8.7 kW generator was split equally to feed two cavities. Mobile temperature sensors (PicoVACQ, TMI-Orion, Castelnau-le-Lez, France) were

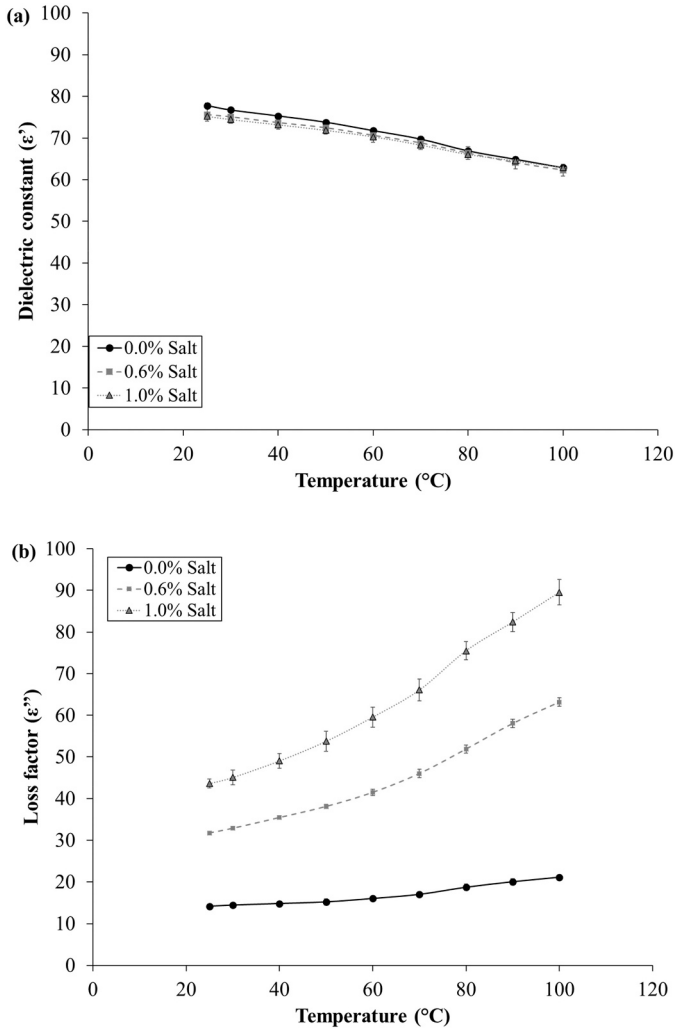

Fig. 3. Dielectric properties of mashed potato-gellan gum gel model foods with 0, 0.6, and 1.0% salt at 915 MHz. ($n = 3$).

Table 1
Process conditions of MAPS for experimental validation.

Process condition	Set value
Generator power [kW]	5/5/8.7
Tray speed [cm/min]	88.9
Pre-heating temperature [°C]	51
Water temperature in MW and holding sections [°C]	91
Cooling temperature [°C]	23
Pre-heating time [min]	45
Holding time [min]	2

placed inside food packages to measure the temperature at the predetermined cold spot location, according to Luan et al. (2015). The resolution of the temperature sensor was ±0.1 °C. Model foods of three different salt levels (0, 0.6, and 1%) and four different thicknesses (22, 24, 27.5, and 36 mm) were processed. Eight trays of the model food placed on a food package carrier were processed in each test run. The vertical position of the model food trays in the metal carrier was adjusted so that the middle layer of the model food was aligned with the central plane of the microwave cavities. After the MAPS processing, the images of different cross-sectional cuts of the model foods were acquired by CCD digital camera (D90, Nikon Inc., Tokyo, Japan) with lens (AFS Nikkor DX 18-70 mm F3.5–4.5, Nikon Inc., Tokyo, Japan). The heating patterns in the cross-sections (x-z plane) inside the samples were determined from images using the computer vision software described by Pandit et al. (2007). Tests were carried out twice at each condition for replication of experiments.

2.3. Penetration depth and J-T number

The microwave penetration depth (D_p) is the distance between the product surface and the location (inside the product) where the microwave power reduces to 36.8%. It was calculated by (Datta, 2001):

$$D_p = \frac{c}{2\pi f\sqrt{2\varepsilon_r'\left[\sqrt{\left(\frac{\varepsilon_r''}{\varepsilon_r'}\right)^2+1}-1\right]}} \tag{10}$$

where c is the speed of light in free space (2.99×10^8 m/s).

A dimensionless J-T (Jain-Tang) number derived by Jain et al. (2019) was used to interpret the maximum heating rates relating to dielectric properties and thickness:

$$J-T\ number = \frac{2\pi\varepsilon_r'' L}{\sqrt{\sqrt{\varepsilon_r'^2+\varepsilon_r''^2}\lambda_{air}}} \tag{11}$$

where λ_{air} is the wavelength of 915 MHz microwaves in the air.

2.4. Statistical analysis

Regression analysis with 95% and 98% confidence intervals was conducted by Excel (version 16.0, Microsoft, Redmond, WA, USA) to validate the analytical model with experimental results. All calculations were performed using Matlab (2017b, MathWorks, Natick, MA, USA) and Excel.

3. Results and discussion

3.1. Comparison of experimental and calculated temperature increase

Based on the measured dielectric properties (shown in Fig. 3) and the volumetric specific heat (ρC_p), the temperature increases (ΔT) at the cold spot in the central layer of the mashed potato-gellan gum model foods with different thicknesses (22, 25, 27.5, and 36 mm) and salt concentrations (0.0, 0.6, and 1.0%) during the microwave heating in MAPS were estimated using the analytical model developed in section 2.1. The dielectric properties of the model foods and ΔT from both calculations and experiments are listed in Table 2. The calculated and experimental ΔT data for the model food samples are close to each other (average difference: 1.9 ± 1.2 °C). The ΔT decreased as the thickness of model foods increased at all salt concentrations.

According to the calculated data, the larger ΔT at the central layer of the 0.6%-salt model foods indicated faster heating rates as compared to that in the 0.0%- and 1.0%-salt model foods of the same thickness, with the exception of the 36-mm thick samples. For the 36-mm thick samples, the 0%-salt sample had the largest ΔT. The calculated ΔT data were slightly smaller than the measured ones for most of the model food samples. This might have been caused by the fact that the calculation did not consider the heat transfer from hot water to food and heat conduction inside the food. The inconsistency in the few data points might be due to the deviations in the measured thickness of individual model food samples. A 0.5 mm difference in thickness could make a difference of 0.34 to 0.94 °C with 2.48 min of microwave heating. The average difference between the experimental and calculated ΔT data was 1.9 ± 1.2 °C. This is acceptable, as the main purpose of the calculations was to evaluate the influence of sample properties and thickness on relative heating rates in the microwave heating section of a MAPS.

The estimated temperature increases correlated well with experimental temperature increases during microwave heating in MAPS

Table 2
Specific properties of model foods and temperature increase during microwave heating at 915 MHz ($n = 2$).

	Dielectric constant*	Loss factor*	Thickness [mm]	Measured temperature increase [°C]**	Estimated temperature increase [°C]	Temperature increase difference [°C]***	J-T number	Penetration depth [mm]
0.0% salt	71.3± 0.6	16.4± 0.3	21.9±0.0	27.0±0.9	24.5±0.1	2.5±0.8	0.82±0.0	26.8±0.5
			24.7±0.2	25.2±1.6	22.5±0.1	2.8±1.4	0.92±0.0	
			26.9±0.4	23.4±0.5	20.8±0.4	2.6±0.1	1.00±0.0	
			35.9±0.2	16.3±2.0	15.7±0.2	0.6±1.8	1.29±0.0	
0.6% salt	66.8±5.8	43.1±1.6	22.1±0.2	33.2±0.8	32.3±0.0	0.9±0.8	2.18±0.0	10.6±0.4
			24.4±0.6	25.9±0.4	27.3±1.0	1.5±0.6	2.34±0.1	
			27.2±0.2	20.2±0.7	23.3±0.3	3.1±0.4	2.44±0.0	
			36.3±0.1	12.2±1.1	14.6±0.0	2.4±1.1	3.13±0.0	
1.0% salt	69.7±0.4	61.4±1.6	22.0±0.1	28.5±0.7	28.2±0.2	0.3±0.5	2.77±0.0	7.7±0.3
			24.5±0.5	24.4±0.7	23.3±0.9	1.1±0.3	3.02±0.1	
			27.1±0.2	17.2±0.5	19.3±0.4	2.1±0.1	3.27±0.0	
			36.6±0.4	10.3±0.9	9.7±0.4	0.6±0.4	3.82±0.6	

* Dielectric property values are the averages of the dielectric property data measured in the temperature range of 50–90 °C.
** Temperature increase during microwave heating after pre-heating.
*** Temperature difference between measured and estimated temperature increase.

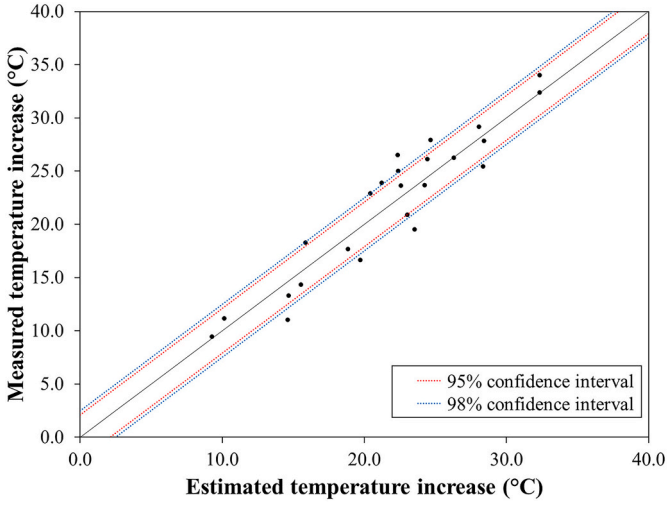

Fig. 4. Comparison of predicted temperature increase by the analytical model and experimental temperature increase of model food with various salt contents and thicknesses in the microwave heating during the MAPS process.

(Fig. 4). Although there were several data points out of the 95% confidence interval, the predicted data mostly differed by less than 2 °C from experimental data, which is within the 98% confidence interval. The R^2 of 0.89 showed a goodness-of-fit of the linear regression in the experimental data. It suggests that the temperature increase during microwave heating could be calculated using the analytical model with the obtained E_{0eff} for the pre-determined cold spot in the package. The reasonably good agreement between the experimental and calculated results also confirms that the analytical model could be an effective tool for estimating temperature increases during microwave heating in MAPS.

3.2. Influences of thickness and salt level of model food on dissipated energy

The dissipated energy along the microwave propagation direction (z-direction) was calculated using the analytical model (Eq. 1) to understand the effect of the thickness (22, 25, 27.5, and 36 mm) and salt concentration (0.0, 0.6, and 1.0%) on the vertical heating pattern within the model foods. As shown in Fig. 5, the in-phase microwaves from the top and bottom waveguides created well-defined nodes and anti-nodes along with the depth (z-direction) in a food package. The dissipated microwave energy in the central layer of the model food decreased, while that at the surface increased, with the increase in the thickness of the model food. For model foods with 0.6% salt content (Fig. 5b), the dissipated energies in the central layer were 776.5, 674.0, 568.3, and 357.4 kW/m^3 for L = 22, 25, 27.5, and 36 mm, respectively. The dissipated energy in the near-surface region increased from 316.4 kW/m^3 for $L = 22$ mm to 644.4 kW/m^3 for $L = 36$ mm. A single peak around the center of the model foods was observed for L = 22 mm, whereas multiple peaks in the center and surface were observed for $L = 27.5$ and 36 mm. Model foods with 0.0 and 1.0% salt content followed the observed trend for model foods with 0.6% salt content. These results also followed the trend in previous research (Jain et al., 2019).

Fig. 5 also clearly illustrates the effect of salt level on microwave power dissipation inside the model food of different thicknesses. For the samples with thicknesses of 22, 25, and 27.5 mm, the model food with 0.6% salt content had a higher energy dissipation in the central layer compared with 0.0 and 1.0% salt content samples. In the 22 mm thick sample, the dissipated power for the 0.0, 0.6, and 1.0% salt level at the central layer (x-z plane) was 600.3, 776.5, and 688.3 kW/m^3, respectively. For the 36-mm thick samples, the model food with 0% salt content had the highest energy dissipation in the central layer. Moreover, the food with 1.0% salt level experienced more surface heating compared with other salt level model foods of the same thickness. A higher salt level (resulting in higher loss factor) could not guarantee higher energy dissipation in the central layer of the food product during microwave heating. The reason is that most of the microwave energy was dissipated at the surface of food due to the shallow penetration depths of the microwaves. Jain et al. (2019) also showed similar results for mashed potatoes, peas, and rice model foods. Appropriate ranges of loss factor of food should be selected by modifying food formulation.

3.3. Comparison of analytical results of energy dissipation with experimental heating patterns

Fig. 6 shows the changes in the heating pattern of model foods with respect to thickness (22, 25, 27.5, and 36 mm) and salt content (0, 0.6, and 1%) on an x-z plane (a vertical cross-section cut along the central line of the sample). The heating pattern images were obtained by using the computer vision method (Pandit et al., 2007) that captured the relative color changes in model foods after the thermal processing in MAPS. The red and blue color indicates the maximum and minimum thermal intensity, respectively, based on formation of M-1 chemical marker in thermal processing. The heating pattern results agreed well with the dissipated microwave energy calculated using the analytical

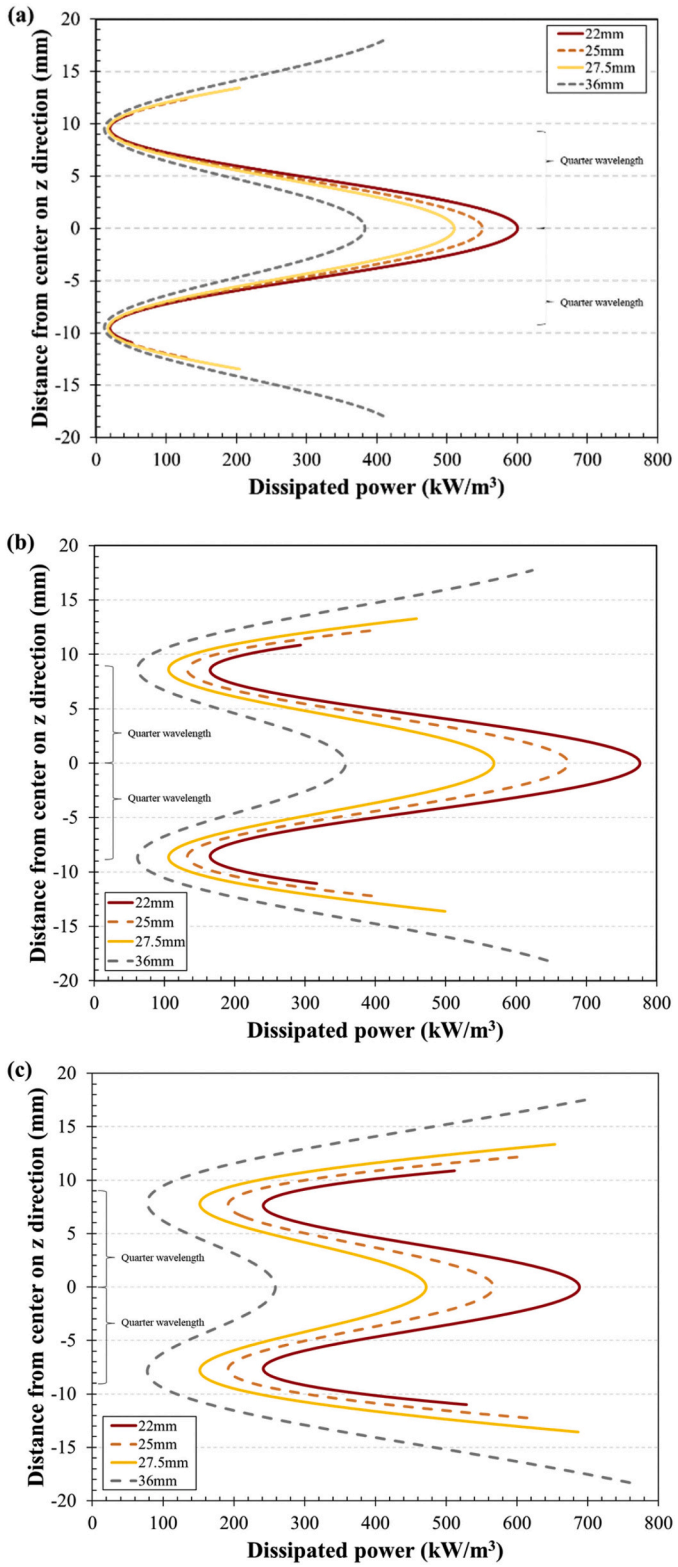

Fig. 5. Effect of food thicknesses and salt contents on dissipated power distribution along the wave propagation direction (z) in a food: (a) 0.0% salt, (b) 0.6% salt, and (c) 1.0% salt.

model (Fig. 5). The hot spots were located at the central layer in the smaller-thickness (22 and 25 mm) samples regardless of salt concentration. The 0%-salt 27.5-mm sample had the hot spot location at the central layer while the 0.6%- and 1.0%-salt 27.5 mm samples experienced surface heating. The 36-mm-thick samples experienced surface heating irrespective of salt level because the thicker model foods limited energy penetration into the central layer. These trends were similar to the analytical results which showed that surface heating increased as the thickness increased.

At every quarter of a wavelength, the node (minimum amplitude) and antinode (maximum amplitude) of the standing wave were located. The antinode was placed on the central layer of the model food, whereas nodes were located a quarter wavelength away (Fig. 5). The cross-sectional heating patterns (Fig. 6) matched the theoretical calculation; the locations of the cold and hot zones (in the x-z plane), as indicated by the color changes in the heating patterns (Fig. 6), agreed with the locations of the antinodes and nodes obtained in the analytical calculation results (Fig. 5).

3.4. Penetration depth and J-T number

Penetration depth generally indicates how microwave energy can penetrate a product. As shown in Table 2, the penetration depth changed with the salt concentration of the model food. For instance, the average penetration depth of the model foods with 0.0, 0.6, and 1.0% salt contents was 26.8, 10.5, and 7.7 mm, respectively. Although 915 MHz microwaves had a relatively deep penetration depth in the 0%-salt model food samples, the heating rates at the cold spot of the 0%-salt samples with different thicknesses were not always higher than that in higher salt content samples. Specifically, the 0.6%-salt sample had 50% less penetration depth, but the heating rate in the sample center layer was higher than in the 0%-salt sample of 22 and 25 mm thickness. With a thickness of 36 mm, the heating rate at the cold spot was higher in the 0%-salt sample (ΔT=15.7 °C) than in the 0.6%- and 1%-salt samples (ΔT=14.6 and 9.7 °C, respectively). But for the model foods of other thicknesses (22, 25 and 27 mm), the heating rates were ΔT=32.3, 27.8, and 23.3 °C, respectively, in the 0.6%-salt samples, and ΔT=24.5, 22.5, and 20.8 °C, respectively, in the 0%-salt samples. The penetration depth only reflects attenuation of the microwave power of the transverse wave by a factor e^{-1} in a product (Sadiku, 2014). In MAPS, microwaves propagated from top and bottom are super-imposed within the microwave cavity, which creates a standing waveform in the z-direction. This was clearly predicted by the analytical model (Eq. 1). Luan et al. (2016) also verified the electric field distribution with a standing wave pattern in the microwave assisted thermal process system using 3D numerical simulation. For this reason, the penetration depth alone could not fully explain the complex phenomena of the propagation of microwaves in MAPS.

The J-T number (Eq. 11) is a dimensionless number developed to explain the correlation between dielectric properties and thicknesses with the heating rate at the cold spot of a food package. The calculated J-T number values for model foods with various thicknesses and dielectric properties are included in Table 2. The J-T number increased with increasing thickness and loss factor. The J-T number at the highest heating and lowest heating rates was 2.18 (22-mm and 0.6%-salt sample) and 3.82 (35-mm and 1%-salt sample), respectively. This result matched with the previously reported data in Jain et al. (2019) which stated that the maximum energy dissipated in the food is within the J-T number range between 1.8 and 2.2. As mentioned in sections 3.1 and 3.2, in a given MATS system or MAPS and with a fixed power setting, heating uniformity and heating rate largely depend on the dielectric properties and thicknesses of foods. For the MAPS processing, the J-T number could be a better indicator to estimate the heating rate than the penetration depth. A process developer could simply assess the heating efficiency by checking the J-T number. If the values are too high or much smaller than the J-T range of 1.8–2.2, the process conditions may need to be adjusted for higher heating efficiency (Jain et al., 2019). Thus, the analytical model combined with the J-T number can be useful in developing processing schedules for MAPS processes. But it is still not a straightforward task for a layperson to use the analytical model. Thus, a simplified chart was developed below.

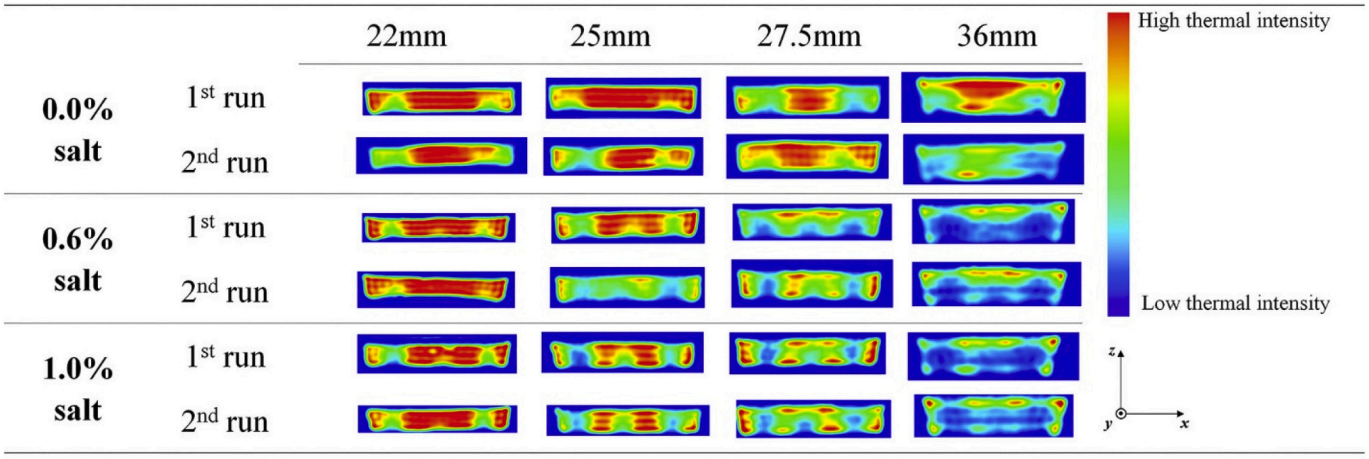

Fig. 6. Heating patterns on the x-z plane (vertical cross-section cut along the central line of the sample) inside mashed potato-gellan gum model food with different salt contents and thicknesses (The images were obtained by using computer vision system that captured color changes in model foods after the thermal processing in MAPS).

3.5. Development of simplified chart

Several methods, such as the General method or the Ball method, have been utilized to develop processing schedules for conventional thermal processes in the food industry (Holdsworth, Simpson, & Barbosa-Cánovas, 2008; Stoforos, 2010). These methods, along with well-established procedures, are very crucial to avert monetary loss and unnecessary trials and errors associated with large scale industrial systems. For the microwave assisted thermal processing, as an emerging technology, there is no standard method to estimate the temperature increase in packaged foods.

The validation results discussed above suggest that the analytical model could be applied to estimate the temperature increase at a cold spot in food products with different thickness or dielectric properties. Based on the analytical model developed in this study, a simplified chart shown in Fig. 7 was developed for estimating temperature increase during microwave heating for the pilot-scale process conditions used in this study. The horizontal axis and vertical axis, respectively, represents the loss factor at the average temperature and the average heating rate (°C/min) during microwave heating. The curves for different-thicknesses of food samples show the relationship between the heating rate, loss factor, and food thickness. The ρC_p of 1 MJ/(m^3·°C) was used for the chart development. For a given food, the chart-value for the heating rate can be found using the loss factor of the food at the average temperature during the microwave heating and the thickness of the food. The heating rate of the food can be obtained by dividing the chart value with the value of the actual ρC_p of the product.

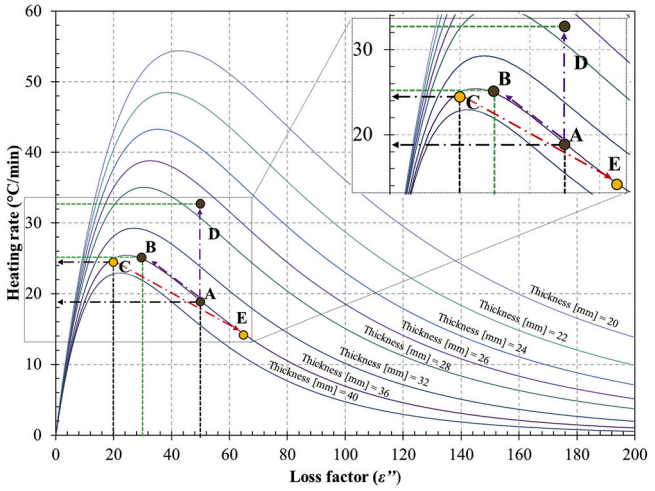

Fig. 7. Example of developed chart for food products with standard volumetric specific heat and dielectric constant (ρC_p=1.0 MJ/(m^3·°C), and $\varepsilon' = 70$) for MAPS processing.

For example, when ground beef steak (ρC_p=3.2 MJ/(m^3·°C) and ε_r''= 50) as the main component of a product is processed in a 36 mm thick package (ASHRAE, 2006), the corresponding point A in Fig. 7 indicates that the estimated value for the heating rate is 19 °C/min for a subject with a ρC_p of 1 MJ/(m^3·°C). The heating rate of the steak that has a ρC_p of 3.2 MJ/(m^3·°C), therefore, is 5.9 °C/min (=19 °C/min divided by 3.2). Thus, if a manufacturer wants to process their food packages from 60 to 90 °C at the cold spot, the food packages should have 5.1 min of resident time in the microwave heating section of the MAPS. When the formulation changes, e.g., by reducing salt, that results in ε_r''= 30, the manufacturer can obtain a higher heating rate of 7.8 °C/min (=25 °C/min divided by 3.2) in the package of the same thickness (B in Fig. 7). The microwave heating time, in this case, should be shortened to 3.9 min for the same temperature rise at the cold spot.

Through reformatting product recipes or changing package thicknesses, the chart can be used to adjust the heating time for processing of not only plain food packages (single-compartment trays or pouches) but also multi-compartment trays filled with different food components. For food recipe development and thickness selection, one needs to consider that the different food components filled in different parts of the multi-compartment trays should have similar heating rates in order to get a uniform and efficient MAPS heating process. If the manufacturer selects carrots (ρC_p=2.3 MJ/(m^3·°C) and ε_r''= 20) as the side to ground beef steak (ρC_p=3.2 MJ/(m^3·°C) and ε_r''= 50) in the same two-compartment tray (ASHRAE, 2006; Tran, Stuchly, & Kraszewski, 1984), the heating rate of carrots would be 10.4 °C/min (=24 °C/min divided by 2.3) (C in Fig. 7), which is much higher than that of the steak (5.9 °C/min, A in Fig. 7). Similar heating rates can be obtained in the two food compartments of the same tray by either reducing the thickness of the steak from 36 to 27 mm (D in Fig. 7), resulting in a heating rate of 10.3 °C/min in the steak (33 °C/min divided by 3.2), or increasing ε_r'' of the carrot by adding more salt (E in Fig. 7), resulting in a heating rate of 6.1 °C/min in the carrots (14 °C/min divided by 2.3).

As demonstrated in the examples presented above, the chart can guide product development (recipe and thickness selection/adjustment) for uniform and efficient heating with various food products that have different ε_r'' and ρC_p values. Better heating uniformity in multi-compartment trays can be obtained by matching the heating rates for

different food components. In industrial applications, this chart may be used as a convenient tool to assess relative heating rates of different food products in different package geometries in a specific industrial microwave system using the 915 MHz single-mode cavity design as depicted in Figs. 1 and 2. With known microwave power applied to each cavity, it can also be used to estimate heating rates of a specific product in a given package. The chart should be adjusted with new E_{0eff} to obtain accurate estimation when the change is made in the microwave power and/or package design. Although the chart was developed based on an analytical model validated with MAPS, it can also be used to estimate temperature rises at the cold spot of pre-packaged foods in MATS processes because of the similarity in the microwave cavity design between MAPS and MATS. The main difference between the two processes is that both the initial and final product temperatures are about 30-40^{o}C higher in a MATS process than in a MAPS process.

The chart was developed using homogenous model foods, but it can provide useful insight to guide the development of process schedules for various non-homogenous food products in MATS and MAPS systems. Basically, all commercial thermal processes, including microwave assisted thermal processes, are developed based on the 'worst-case scenario' (FDA, 2016; IFTPS, 2014). For non-homogeneous foods, process engineers use the temperature history in a food component that has the lowest heating rate at the cold spot in the food packages to develop processing schedules. Thus, our chart can be used to estimate the heating rate and select an approximate range of processing time, assuming that the packages are filled with the same food component as the worst-case. The process conditions can then be refined by directly measuring the temperature of the cold spot in food packages using mobile sensors as described in Luan et al. (2015), Tang (2015), and Tang et al. (2018).

This is our first attempt to develop a simplified chart to assist food companies in developing a process schedule for industrial production of shelf-stable (using MATS) or chilled (using MAPS) pre-packaged meals. Further research is needed to refine, validate, and expand the chart for a wide range of products of interest to the food industry. For example, the influence of dielectric constant is not included in the chart. But based on previous studies, the values of dielectric constant of most high moisture food components fall into a narrow range (e.g., ε_r' changed from 80 to 70 when sugar contents were increased by 30%) (Jain et al., 2019; Luan, Tang, Pedrow, Liu, & Tang, 2015; Wang, Tang, Liu, & Bohnet, 2018; Zhang et al., 2015). Thus, this chart can still be applicable to those foods. Additional supplementary charts could be developed for the food components having extremely high or low dielectric constants.

4. Conclusions

An analytical model was used to estimate the temperature increase at the cold spot inside food packages during microwave heating in MAPS. It was validated using experimental results from pilot-scale testing of the model foods with various salt concentrations and thicknesses. The calculated temperature increases in the model foods based on the analytical model were in general agreement with the experimental results. Results of the validation also conclude that the J-T number can be an energy-efficiency indicator to determine the process parameters for processing food products with different dielectric properties and thicknesses. A user-friendly chart was developed from analytical calculations to visually represent the relationship between heating rates, dielectric loss factors, and package thicknesses. This chart can potentially help food product developers and processors to optimize food recipes and process schedules for MAPS processing of their food products.

Declaration of Competing Interest

- All authors have participated in (a) conception and design, or analysis and interpretation of the data; (b) drafting the article or revising it critically for important intellectual content; and (c) approval of the final version.
- This manuscript has not been submitted to, nor is under review at, another journal or other publishing venue.
- The authors have no affiliation with any organization with a direct or indirect financial interest in the subject matter discussed in the manuscript

Acknowledgments

This research was supported by the (USDA)National Institute of Food and Agriculture Research grants number 2016-68003-24840, Hatch project #1016366, and Washington State University Agriculture Research Center.

References

American Society of Heating and Air-Conditioning Engineers (ASHRAE). (2006). Chapter 9–thermal properties of foods. In *ASHRAE Handbook—Refrigeration*. ASHRAE.

Ayappa, K. G., Davis, H. T., Crapiste, G., Davis, E. A., & Gordon, J. (1991). Microwave heating: An evaluation of power formulations. *Chemical Engineering Science, 46*(4), 1005–1016. https://doi.org/10.1016/0009-2509(91)85093-D

Bornhorst, E. R., Tang, J., Sablani, S. S., & Barbosa-Cánovas, G. V. (2017). Development of model food systems for thermal pasteurization applications based on Maillard reaction products. *LWT - Food Science and Technology, 75*, 417–424. https://doi.org/10.1016/j.lwt.2016.09.020

Bornhorst, E. R., Tang, J., Sablani, S. S., Barbosa-Canovas, G. V., & Liu, F. (2017). Green pea and garlic puree model food development for thermal pasteurization process quality evaluation. *Journal of Food Science, 82*(7), 1631–1639. https://doi.org/10.1111/1750-3841.13739

Chandrasekaran, S., Ramanathan, S., & Basak, T. (2013). Microwave food processing—A review. *Food Research International, 52*(1), 243–261. https://doi.org/10.1016/j.foodres.2013.02.033

Chen, H., Tang, J., & Liu, F. (2006). Coupled simulation of an electromagnetic heating process using the finite difference time domain method. *Journal of Microwave Power and Electromagnetic Energy, 41*(3), 50–68. https://doi.org/10.1080/08327823.2006.11688563

Chen, H., Tang, J., & Liu, F. (2008). Simulation model for moving food packages in microwave heating processes using conformal FDTD method. *Journal of Food Engineering, 88*(3), 294–305. https://doi.org/10.1016/j.jfoodeng.2008.02.020

Datta, A. K. (2001). *Handbook of microwave technology for food application*. CRC Press.

Dolores Alvarez, M., Herranz, B., Campos, G., & Canet, W. (2017). Ready-to-eat chickpea flour purée or cream processed by hydrostatic high pressure with final microwave heating. *Innovative Food Science & Emerging Technologies, 41*, 90–99. https://doi.org/10.1016/j.ifset.2017.02.011

FDA. (2016). Center for Food Safety and Applied Nutrition. *Hazard Analysis and Risk-Based Preventive Controls for Human Food: Guidance for Industry*. Department of Health and Human Services.

Holdsworth, S. D., Simpson, R., & Barbosa-Cánovas, G. V. (2008). *Thermal Processing of Packaged Foods*. Springer.

Hossan, M. R., Byun, D., & Dutta, P. (2010). Analysis of microwave heating for cylindrical shaped objects. *International Journal of Heat and Mass Transfer, 53*(23), 5129–5138. https://doi.org/10.1016/j.ijheatmasstransfer.2010.07.051

Huang, L., & Sites, J. (2010). New automated microwave heating process for cooking and pasteurization of microwaveable foods containing raw meats. *Journal of Food Science, 75*(2), E110–E115. https://doi.org/10.1111/j.1750-3841.2009.01482.x

IFTPS. (2014). *Guidelines for Conducting Thermal Processing Studies. 2020*.

Jain, D., Tang, J., Liu, F., Tang, Z., & Pedrow, P. D. (2018). Computational evaluation of food carrier designs to improve heating uniformity in microwave assisted thermal pasteurization. *Innovative Food Science & Emerging Technologies, 48*, 274–286. https://doi.org/10.1016/j.ifset.2018.06.015

Jain, D., Tang, J., Pedrow, P. D., Tang, Z., Sablani, S., & Hong, Y.-K. (2019). Effect of changes in salt content and food thickness on electromagnetic heating of rice, mashed potatoes and peas in 915 MHz single mode microwave cavity. *Food Research International, 119*, 584–595.

Joyner, H. S., Jones, K. E., & Rasco, B. A. (2016). Microwave pasteurization of cooked pasta: Effect of process parameters on texture and quality for heat-and-eat and ready-to-eat meals. *Journal of Food Science, 81*(6), E1447–E1456. https://doi.org/10.1111/1750-3841.13334

Luan, D., Tang, J., Pedrow, P. D., Liu, F., & Tang, Z. (2013). Using mobile metallic temperature sensors in continuous microwave assisted sterilization (MATS) systems. *Journal of Food Engineering, 119*(3), 552–560. https://doi.org/10.1016/j.jfoodeng.2013.06.003

Luan, D., Tang, J., Pedrow, P. D., Liu, F., & Tang, Z. (2015). Performance of mobile metallic temperature sensors in high power microwave heating systems. *Journal of Food Engineering, 149*, 114–122. https://doi.org/10.1016/j.jfoodeng.2014.09.041

Luan, D., Tang, J., Pedrow, P. D., Liu, F., & Tang, Z. (2016). Analysis of electric field distribution within a microwave assisted thermal sterilization (MATS) system by computer simulation. *Journal of Food Engineering, 188*, 87–97. https://doi.org/10.1016/j.jfoodeng.2016.05.009

Luan, D., Wang, Y., Tang, J., & Jain, D. (2017). Frequency distribution in domestic microwave ovens and its influence on heating pattern. *Journal of Food Science, 82*(2), 429–436. https://doi.org/10.1111/1750-3841.13587

Moreno-Vilet, L., Hernández-Hernández, H. M., & Villanueva-Rodríguez, S. J. (2018). Current status of emerging food processing technologies in Latin America: Novel thermal processing. *Innovative Food Science & Emerging Technologies, 50*, 196–206. https://doi.org/10.1016/j.ifset.2018.06.013

Orsat, V., Raghavan, G., & Krishnaswamy, K. (2017). Microwave technology for food processing: An overview of current and future applications. In *The Microwave Processing of Foods* (pp. 100–116). Elsevier.

Pandit, R. B., Tang, J., Liu, F., & Mikhaylenko, G. (2007). A computer vision method to locate cold spots in foods in microwave sterilization processes. *Pattern Recognition, 40*(12), 3667–3676.

Peng, J., Tang, J., Barrett, D. M., Sablani, S. S., Anderson, N., & Powers, J. R. (2017). Thermal pasteurization of ready-to-eat foods and vegetables: Critical factors for process design and effects on quality. *Critical Reviews in Food Science and Nutrition, 57*(14), 2970–2995. https://doi.org/10.1080/10408398.2015.1082126

Resurreccion, F. P., Luan, D., Tang, J., Liu, F., Tang, Z., Pedrow, P. D., & Cavalieri, R. (2015). Effect of changes in microwave frequency on heating patterns of foods in a microwave assisted thermal sterilization system. *Journal of Food Engineering, 150*, 99–105. https://doi.org/10.1016/j.jfoodeng.2014.10.002

Resurreccion, F. P., Tang, J., Pedrow, P., Cavalieri, R., Liu, F., & Tang, Z. (2013). Development of a computer simulation model for processing food in a microwave assisted thermal sterilization (MATS) system. *Journal of Food Engineering, 118*(4), 406–416. https://doi.org/10.1016/j.jfoodeng.2013.04.021

Sadiku, M. N. O. (2014). *Elements of Electromagnetics*. Oxford University Press Inc.

Soto-Reyes, N., Temis-Pérez, A. L., López-Malo, A., Rojas-Laguna, R., & Sosa-Morales, M. E. (2015). Effects of shape and size of agar gels on heating uniformity during pulsed microwave treatment. *Journal of Food Science, 80*(5), E1021–E1025. https://doi.org/10.1111/1750-3841.12854

Stoforos, N. G. (2010). Thermal process calculations through Ball's original formula method: A critical presentation of the method and simplification of its use through regression equations. *Food Engineering Reviews, 2*(1), 1–16. https://doi.org/10.1007/s12393-010-9014-4

Tang, J. (2015). Unlocking potentials of microwaves for food safety and quality. *Journal of Food Science, 80*(8), E1776–E1793. https://doi.org/10.1111/1750-3841.12959

Tang, J., Hong, Y.-K., Inanoglu, S., & Liu, F. (2018). Microwave pasteurization for ready-to-eat meals. *Current Opinion in Food Science, 23*. https://doi.org/10.1016/j.cofs.2018.10.004

Tran, V., Stuchly, S., & Kraszewski, A. (1984). Dielectric properties of selected vegetables and fruits 0.1-10.0 GHz. *Journal of Microwave Power, 19*(4), 251–258. https://doi.org/10.1080/16070658.1984.11689372

Van Remmen, H. H., Ponne, C. T., Nijhuis, H. H., Bartels, P. V., & Kerkhof, P. J. (1996). Microwave heating distributions in slabs, spheres and cylinders with relation to food processing. *Journal of Food Science, 61*(6), 1105–1114. https://doi.org/10.1111/j.1365-2621.1996.tb10941.x

Wang, Y., Wig, T. D., Tang, J., & Hallberg, L. M. (2003). Dielectric properties of foods relevant to RF and microwave pasteurization and sterilization. *Journal of Food Engineering, 57*(3), 257–268. https://doi.org/10.1016/S0260-8774(02)00306-0

Wang, J., Tang, J., Liu, F., & Bohnet, S. (2018). A new chemical marker-model food system for heating pattern determination of microwave-assisted pasteurization processes. *Food and Bioprocess Technology, 11*(7), 1274–1285. https://doi.org/10.1007/s11947-018-2097-2

Yang, H. W., & Gunasekaran, S. (2001). Temperature profiles in a cylindrical model food during pulsed microwave heating. *Journal of Food Science, 66*(7), 998–1004. https://doi.org/10.1111/j.1365-2621.2001.tb08225.x

Zhang, W., Luan, D., Tang, J., Sablani, S. S., Rasco, B., Lin, H., & Liu, F. (2015). Dielectric properties and other physical properties of low-acyl gellan gel as relevant to microwave assisted pasteurization process. *Journal of Food Engineering, 149*, 195–203.